Structure and Dynamics of Orientational Defects in Ice

R. Podeszwa

Quantum Chemistry Laboratory, Department of Chemistry, University of Warsaw, Pasteura 1, 02-093 Warsaw, Poland

V. Buch

The Fritz Haber Institute for Molecular Dynamics, The Hebrew University, Jerusalem 91904, Israel

Orientational defects play an important role in a variety of ice phenomena, such as dielectric and mechanical relaxation, and electrical conductivity. In this study, structure and migration mechanisms of such defects were investigated using molecular dynamics simulations. Defect structure is quite different from the one proposed originally by Bjerrum [Science **115**, 385 (1952)]. Two basic structures were identified for the D defect (with excess OH in the network), and one dominant structure was obtained for the L defect (with a missing hydrogen bond). Typically, one water molecule in a defect is displaced ≈ 1 Å from the crystal lattice site. Defect jumps occur via vibrational phase coincidence.

PACS numbers: 66.30.Lw

Water ice is one of the most important natural substances. The common crystalline form of solid H_2O (ice Ih) can be viewed as a nearly perfect tetrahedral network of H bonds [1,2]. The four hydrogen bonds effectively immobilize each water molecule. Therefore, ice properties related to transport and relaxation are believed to be dominated by defects. This Letter addresses the structure and the dynamics of the kind of defects that promote molecular reorientation, e.g., during dielectric and mechanical relaxation [1]. Such defects play also an important role in the unusual electrical conductivity of ice [1], and perhaps in the crystallization of icy substances [3].

While there is little doubt about the existence and the importance of defects, their molecular structures and migration mechanisms are far from being well understood. A classical model which has been broadly invoked in the past was suggested by Bjerrum [4] (see Fig. 1). The model postulated the existence of two kinds of orientational defects, formed by rotation of an OH bond away from its own hydrogen bond axis, into that of a neighbor. One pair of neighboring $O \cdots O$ atoms is left with no intervening H atom (an L defect), while a pair of OH bonds are facing each other ($OH \cdots HO$) along another near neighbor $O \cdots O$ axis (a D defect). A jump of a defect to a new site occurs by a 120° rotation of a molecule, as shown in Fig. 1. Such jumps were proposed to provide a mechanism for molecular reorientation. The defects diffuse in ice until a recombination of an L-D pair takes place.

However, it has been clear that the Bjerrum model cannot be correct beyond a cartoon level. Electrostatic repulsion between partial positive charges on the H atoms of the D defect and between partial negative charges of the L defect is bound to alter the defect structure. Previous studies of *relaxed* ice defects [5] focused mostly on energy minimization of reduced dimensionality models which included a defect and neighboring molecules [1,2,5]. These investigations produced a variety of results, depending on the choice of "important" relaxing coor-

dinates. In an alternative one-dimensional kink-solitonic model of orientational defects, the defects were proposed to be delocalized over numerous water molecules [6].

Here, we employ molecular dynamics simulations of defects in a realistic ice model containing several hundred
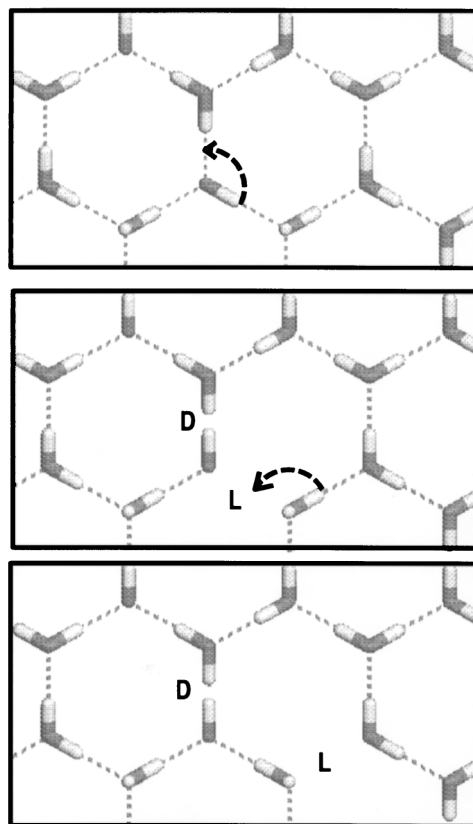

FIG. 1. From top to bottom: schematic representation of the formation of a pair of D and L defects, and an L-defect jump, in the Bjerrum model. The c axis is perpendicular to the page. The second OH of the rotating molecule in the top (middle) panel points into (out of) the page, respectively.

molecules. The model is sufficiently large to investigate, for the first time, structure and dynamics of *migrating* orientational defects in ice at finite temperatures.

The ice structure. — Ice Ih is orientationally disordered, despite the nearly perfect tetrahedral network of hydrogen bonds [1,2]. That is, while O atoms form a nearly perfect periodic pattern [7], the H atoms are arranged at random within the constraints of the so–called ice rules—two chemically bonded and two hydrogen bonded H atoms around each O atom. Our method to generate orientationally disordered ice models is described in Ref. [8]. The present study employs a rectangular ice model containing 360 water molecules; several check-up runs employed a larger 1600 molecule model. Periodic boundary conditions were used.

The potential. — The calculation employed an empirical polarizable potential denoted EMP [8], which is a modified version of a potential proposed in Ref. [9]. The modification was carried out by us recently [8], in an effort to provide a balanced description of all water phases (solid, liquid, and clusters). Another set of simulations was carried out with the nonpolarizable (and much more computationally efficient) TIP4P potential [10]. The main conclusions of this study were found to be valid for both potentials.

Initial conditions, technical details. — The study does *not* consider the formation mechanism of the defect pair. This is since defect pair formation is associated with a substantial energy barrier [1,2], and is therefore unlikely to be observed on an ordinary simulation time scale. We adopted the basic Bjerrum's assumption, that an orientational defect is associated with one extra or one missing OH bond in the hydrogen bond network. The starting point is an ice structure, with a pair of idealized Bjerrum defects. The ideal *L-D* defect pair was introduced by a rotation of one of the molecules; the two defects were then displaced from each other by a geometric transformation corresponding to 10–13 "ideal" Bjerrum jumps of the *L* defect (see Fig. 1). Conjugate gradient minimization was then applied to this initial structure, followed by heating to a temperature in the range 100–230 K. Finally, a classical trajectory simulation was carried out. The results described below are based mostly on five 20 ps trajectories employing EMP, at 230 K, and twelve 15 ps trajectories employing TIP4P, at 210 K. Two backup calculations (employing EMP and TIP4P, respectively) were 100 ps long. Computational details of classical molecular dynamics are similar to the ones used in our past ice simulations [11,12].

Results. — Three basic defect structures were identified, two derived from *D*, and one from *L*. The structures are shown in Figs. 2 and 3, together with the respective defect jump mechanisms, and some energetics [13]. The two basic structures derived from *D* are very different from the Bjerrum model [see Figs. 2(a) and 3(a)]. The *D* structure as proposed by Bjerrum (see Fig. 1) was
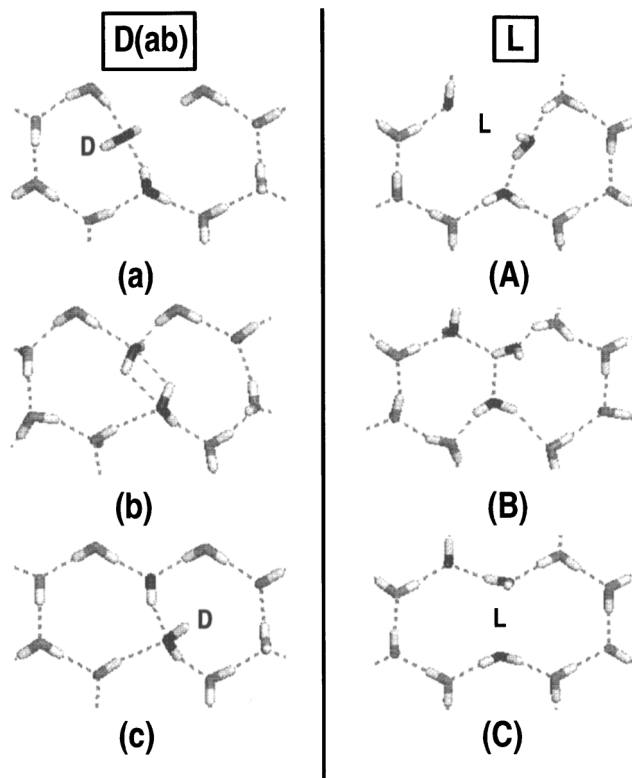

FIG. 2. A jump of a $D(ab)$ defect (left), and of an L defect (right). Snapshots from 230 K trajectories employing EMP. The initial, intermediate, and final states are shown from top to bottom, as projections on the ab plane. For clarity, the initial and the final states were minimized. "D" and "L" denote the locations of the defect. While the figure shows jumps in an ab plane, similar jumps occur between planes. The mean energy of the two D and L defect molecules in (a) and (A) is -11.5 and -9.4 kcal/mol, respectively. The mean molecular energy away from the defects is -13.6 kcal/mol. Only molecules near the plane of the defects are shown.

never found, even as a transition state. The L defect is substantially distorted with respect to the Bjerrum structure. However, in the discussion below, we retain the classical terminology (L and D) as bookkeeping devices, denoting entities with a missing and an extra OH bond, respectively. In the two D defects, the extra OH is oriented either close to the ab hexagonal plane, or close to the c axis; the two species are therefore labeled $D(ab)$ and $D(c)$, respectively. It should be realized that defect structures are influenced by the microscopic neighborhood, which varies because of the orientational disorder. Because of that, there is some variability in the three prototype geometries. However, the three basic structures are easily identifiable throughout the simulations. Typically, each defect contains one molecule which is displaced significantly (≈ 1 Å) from its ideal lattice site.

The D defects. — In the $D(ab)$ defect, shown in Fig. 2(a), the excess OH (denoted D) points into a cavity in the ice structure, and is close to the ab plane. The corresponding water molecule is displaced from its lattice
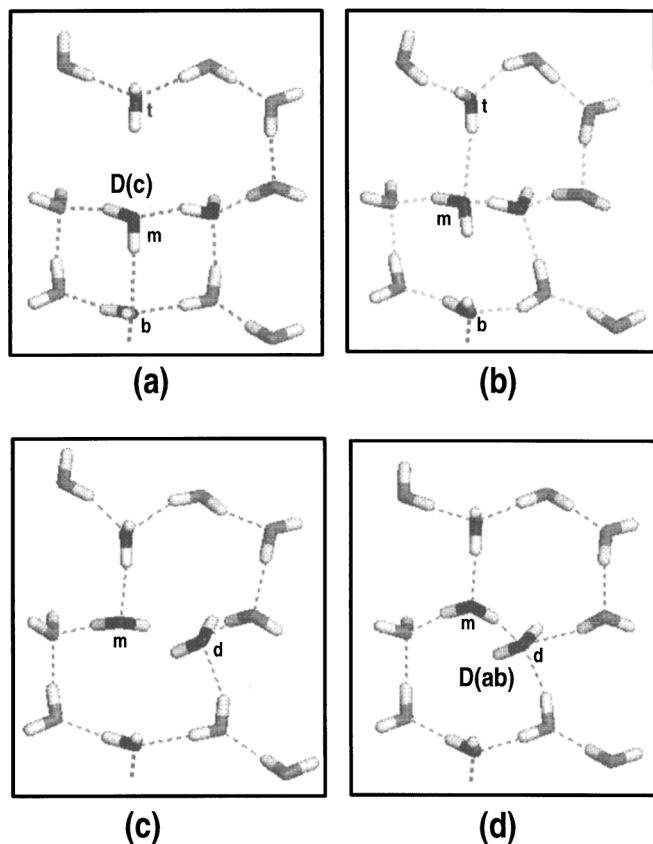
FIG. 3. A jump, in which a $D(c)$ defect is converted into $D(ab)$. Snapshots from a 230 K trajectory employing EMP. For clarity, the initial and the final states were minimized. The c axis is vertical. "$D(c)$" and "$D(ab)$" denote the initial and the final locations of the defect. The energies of the t, m, and b molecules in (a) are -11.3, -13.2, and -14.6 kcal/mol, respectively. Only molecules near the plane of the defects are shown.

site into the cavity, in the direction of the dangling OH. (If this molecule retained its crystal location, significant repulsion would be present between the dangling H, and the neighboring H atoms in the hydrogen bond network.) The displacement at the local minimum energy configuration is in the range 0.8–1.4 Å, and is sufficiently large to break (or weaken considerably) the hydrogen bond with the water molecule on the other side of the dangling OH. The corresponding $O \cdots O$ distance is 3.4–4.0 Å, as compared to the mean minimum $O \cdots O$ distance of 2.785 Å for hydrogen bonds in ice in the EMP potential. Thus, in the limit of long displacement [Fig. 2(a)], this defect can be considered composed of two three-coordinated water molecules, each with one dangling OH, two bonds through O, and one through H. In the limit of short displacement [Fig 2(c)], the defect can be viewed as localized on a single molecule with one hydrogen bond through H, three hydrogen bonds through O (one long), and one dangling OH.

The $D(c)$ form of the D defect, exemplified in Fig. 3(a), was encountered less commonly than $D(ab)$.

$D(c)$ constituted about $1/6$ of the D defects examined in EMP, and about $1/3$ in TIP4P. $D(c)$ is delocalized over three molecules (denoted t, m, and b), which are stacked above each other along the c axis [see Fig. 3(a)]. The middle molecule m is the carrier of the excess OH, which is oriented downwards close to the c axis.

In order to explain the existence of $D(c)$, let us consider as a starting point a structure such as the one shown in Fig. 3(b). This is how the $D(c)$ defect would have looked, if it had chosen to adopt a structure analogous to $D(ab)$; then the excess OH would have pointed into a cavity, in the direction close to the c axis. However, the bottom molecule (denoted b in the figure) attracts the excess OH, resulting in the formation of a new hydrogen bond $m \cdots b$, as seen in the minimum energy structure in Fig. 3(a). At the same time, the m molecule is displaced ≈ 1 Å from its lattice site, and the bond to the top molecule t is "broken." (There is, of course, attractive interaction between m and t; however, the corresponding $O \cdots O$ distance at the minimum is long, in the range 3.7–4.0 Å.)

Defect motion is very efficient, and depends on phase coincidence. A jump $D(ab)$-$D(ab)$ is shown in Figs. 2(a)–2(c). A jump $D(c)$-$D(ab)$ is shown in Fig. 3. A molecule with the excess OH performs high amplitude (≈ 1 Å) oscillations around its minimum, which is displaced from the ideal lattice site. However, every ≈ 0.5 ps the distance of the O atom of the defect H_2O from its lattice site is at the minimum. The jump occurs when the oxygen of the defect molecule approaches its ideal lattice site, while an oxygen of a neighboring molecule performs an excursion away from its lattice site towards a location appropriate for a defect. In the $D(ab)$-$D(ab)$ transition, an exchange between a bonded and a dangling OH occurs, when the O configuration at the neighboring sites becomes roughly equivalent from the point of view of the H atoms [see Fig. 2(b)]. (Sometimes, the second OH of the defect molecule becomes involved in the defect jump, and acquires a new partner in the process.) The asymmetric $D(c)$-$D(ab)$ transition shown in Fig. 3 is somewhat more complex; first the m molecule returns close to its lattice site while breaking the m-b bond and reforming the m-t bond [Figs. 3(a) and 3(b)], after which the m-d bond is broken and the dangling-bonded OH exchange occurs [Figs. 3(b)–3(d)]. Note that half of the molecules can accept both $D(ab)$ and $D(c)$ defects, and half can accept only $D(ab)$; the latter correspond to H_2O with one of the OH bonds aligned along the c axis.

We are not aware of any past reports of $D(ab)$ and $D(c)$ defect structures, as shown in Figs. 2(a) and 3(a). Some past studies [5(b),5(e)] proposed relaxed D structures similar to the variant of $D(ab)$ shown in Fig. 2(c). Other past models [also based on reduced dimensionality minimizations [5(a),5(d)]] proposed relaxed D structures similar to the intermediate state in Fig. 2(b).

The L defect.—The L defect [shown in Figs. 2(A) and 2(C)] is more similar to the Bjerrum model, and

corresponds, in fact, to a single missing hydrogen bond. However, the $O \cdots O$ distance increases dramatically due to electrostatic repulsion. Thus the L defect $O \cdots O$ distance at the minimum is typically about 4 Å; for comparison, in the EMP potential the mean first and second nearest neighbor distances are 2.785 and 4.55 Å, respectively [14]. As a result of the $O \cdots O$ bond lengthening, either one of the defect molecules or both stick out of their normal crystalline positions, into neighboring cavities. The potential surface is very flat in this region, so one may observe an L defect gliding between all three possible configurations during its lifetime at a given site. In calculations employing the polarizable potential, the dipole of the defect pair molecules at the minimum is reduced by ≈ 0.2 D with respect to the mean crystalline value of 2.8 D [8].

The $O \cdots O$ distance in L defects performs a slow high amplitude oscillation (of a period of about 0.5 ps, and an amplitude of ≈ 1 Å). When the distance is close to the minimum, but still contracting, a defect jump may occur, provided that a neighboring hydrogen bonded $O \cdots O$ distance is at the same length as the defected one, and is expanding [see Fig. 2(B)]. The jump occurs by a quick OH rotation at the time when the $O \cdots O$ distances are approximately equal. Typically, a jump occurs after several oscillations of the $O \cdots O$ distance in the defect, but sometimes after one oscillation only.

It is clear that defect dynamics requires further study. Microscopic neighborhood of the defect affects the dynamics; and the number of possible configurations is large, due to the orientational disorder. The number of sites visited by a defect during a 20 ps EMP trajectory at 230 K is in the range 2–11. The number of jumps is usually significantly larger, since back-and-forth transitions occur commonly between the same sites. The defect motion cannot be described as random diffusion between all available sites; rather, preferred paths are present. A defect seems to drift through ice, while getting trapped at some preferential sites, and performing excursions around these sites. The time spent at the "trap sites" is typically several picoseconds [15], but may be as long as a few tens of picoseconds. About 1/5 of the time, defects are found at short lifetime sites, of a duration of ≈ 1 ps. Not uncommonly a double jump occurs, in which a defect is displaced by two lattice sites over a period of a fraction of a picosecond.

The barrier for both L and D defect migration is low. Defect migration on a time scale of picoseconds was observed at $T = 200 - 230$ K for both potentials. For TIP4P, preliminary results were obtained for lower temperatures as well. At 150 K, defect jumps were observed on a time scale of several tens of picoseconds. At 100 K, no significant defect migration was observed in a 500 ps trajectory.

In summary, a new molecular level description was presented for the structures and the migration mechanisms of orientational defects in ice.

[1] P. V. Hobbs, *Ice Physics* (Clarendon, Oxford, 1974).

[2] D. Eisenberg and W. Kauzmann, *The Structure and Properties of Water* (Oxford University Press, New York, 1969).

[3] J. P. Devlin, Int. Rev. Phys. Chem. **9**, 29 (1990).

[4] N. Bjerrum, Science **115**, 385 (1952).

[5] (a) M. Cohan, M. Cotti, J. V. Iribarne, and M. Weissman, Trans. Faraday Soc. **58**, 490 (1962); (b) J. D. Dunitz, Nature (London) **197**, 860 (1963); (c) D. Eisenberg and C. A. Coulson, Nature (London) **199**, 368 (1963); (d) R. Hassan and E. S. Campbell, J. Chem. Phys. **97**, 4326 (1992); (e) P. L. Plummer, in *Physics and Chemistry of Ice,* edited by N. Maeno and T. Hondoh (Hokkaido University Press, Sapporo, 1992), p. 54.

[6] E. S. Kryachko, Chem. Phys. Lett. **141**, 346 (1987).

[7] W. F. Kuhs and M. S. Lehmann, Water Sci. Rev. **2**, 1 (1986).

[8] V. Buch, P. Sandler, and J. Sadlej, J. Phys. Chem. B **102**, 8641 (1998).

[9] S. Kuwajima and A. Warshel, J. Phys. Chem. **94**, 460 (1990).

[10] W. L. Jorgensen, J. Chandrasekhar, J. D. Madura, R. W. Impey, and M. L. Klein, J. Chem. Phys. **79**, 926 (1983).

[11] H. Witek and V. Buch, J. Chem. Phys. **110**, 3168 (1999).

[12] In TIP4P simulations, a potential cutoff of 10 Å was used. The correction for the resulting lack of energy conservation was carried out every 0.1 ps, by rescaling the velocities. For EMP, a cutoff of 10 Å was employed, in conjunction with the reaction field method to account for the long range forces [M. P. Allen and D. J. Tildesley, *Computer Simulations of Liquids* (Clarendon Press, Oxford, 1987), Chap. 5]. A high frequency value of the ice dielectric constant (3.1) was used.

[13] Molecular energy is defined as half the sum of interaction energies with all other molecules within the cutoff.

[14] In a minority of the L configurations, the $O \cdots O$ distance is smaller, around 3.5 Å.

[15] H_2O reorientation on a time scale of picoseconds was also obtained by K. Koga and H. Tanaka, J. Chem. Phys. **104**, 263 (1996), in a simulation of clathrate hydrates at 253 K.